ELSEVIER

S0032-3861(97)00027-X

Polymer Vol. 38 No. 13, pp. 3409–3416, 1997

0032-3861/97/$17.00 + 0.00

polymer communications

Memory effect on spinodal decomposition: 2. Further analysis on effect of uniaxial compression

Tatsuo Izumitani* and Takeji Hashimoto†

Department of Polymer Chemistry, Graduate School of Engineering, Kyoto University, Kyoto 606-01, Japan

(Received 30 September 1996; revised 5 December 1996)

Effects of uniaxial compression on the spinodal decomposition (SD) process of a binary mixture of poly(styrene-*ran*-butadiene) (SBR) and polybutadiene (PB) were studied by using time-resolved light scattering. A given uniaxial compression was imposed on the films which were first subjected to the isothermal demixing at 60°C for various times t_i. Then time changes in the scattering profiles after the compression were observed at 60°C. After the compression, the scattering vector at the maximum scattered intensity in a direction perpendicular to the compression axis q_m was found to decrease abruptly nearly in accord with affine deformation. In an earlier time after the compression, the vector q_m remained unchanged with time for a certain period; sometime after the compression (defined as t_{comp}), the value q_m became identical with that observed for the SD processes in the undeformed films and then decreased with time in the same way as that observed for the undeformed films, revealing that a memory effect of the uniaxial compression decays with time during the time evolution process. The Cahn's linear analysis after the uniaxial compression revealed that the growth rate $R(q)$ of the concentration fluctuations with wave number q depends on t_i, indicating that the SD after the uniaxial compression depends on the initial condition set up by the time t_i and the given compression deformation. These two results on q_m and $R(q)$ illustrate the non-linear nature of the dynamics of the SD process. The scaled structure factors studied as a function of t_i indicated that they were almost identical to that found for the undeformed case. © 1997 Elsevier Science Ltd.

(Keywords: polymer blends; spinodal decomposition; phase-separation kinetics)

Introduction

The ordering process of polymer mixtures via spinodal decomposition (SD) is described by a nonlinear time evolution equation such as the time-dependent Ginzburg–Landau equation. Explorations of the intrinsically nonlinear nature of the dynamical process should be one of the most important themes in this field. The nonlinear nature may be illustrated by studying effects of initial conditions on SD.

Recently we reported the effects of the uniaxial compression on SD in a mixture of polybutadiene (PB) and poly(styrene-*ran*-butadiene) (SBR) (designated hereafter PB/SBR)[1‡] in order to explore the effects of initial conditions. In this study, we tried to control the initial conditions of the specimens in the following way: we first developed a phase separated structure corresponding to an intermediate stage SD, imposed uniaxial compression of various compression ratios γ_p to the specimens and then studied the SD after the compression. In this way we can generate, as the initial conditions, various types of concentration fluctuations with different amplitudes and length scales. Here γ_p is defined as a ratio of the sample thickness after (d) and before the compression (d_0),

$$\gamma_p \equiv d/d_0 \tag{1}$$

We obtained the following two major results: (i) the memory of the initial conditions ('memory effects') decay with time in the intriguing fashion as reported[1]; (ii) the growth rate $R(q;T)$ of a Fourier mode of the concentration fluctuations with wave number q at a phase separation temperature T depends on the initial conditions, and growth of new modes is strongly coupled with that of existing modes.

In this work, we further extend the work along this line to confirm our previous results. Here we controlled the initial conditions in a different way. We first induce the SD to the system for various periods of time t_i which generate phase-separated structures corresponding to early-to-intermediate stage SD and then impose a given compression deformation of $\gamma_p = 1/2$ to the system. In this way we can set intial conditions different from those in the previous work and study their effects on further SD processes. The various stages of SD as described above will be briefly summarized below.

The coarsening process of our polymer mixtures with a critical composition can be classified into the following three stages[2]: (i) early stage, (ii) intermediate stage and (iii) late stage. In the early stage of SD, the time evolution of concentration fluctuations is well described by the linearized theory proposed by Cahn for small molecule systems[3], and the concentration fluctuations grow

* Present address: Daicel Chemical Ind. Ltd, 1239 Shinzaike Aboshi-ku, Himeji, Hyogo 671-12, Japan
† To whom correspondence should be addressed
‡ It should be noted that the effects of shear deformation on further progress of SD was studied by Izumitani and Hashimoto in order to explore the effects of initial conditions; Izumitani, T. and Hashimoto, T., in *Flow-Induced structure in Polymers*, ed. A. I. Nakatani and M. D. Dadmun, ACS Symposium Series 597, 1995, p. 122

exponentially with time. In the intermediate stage of SD, the time evolution of the concentration fluctuations becomes increasingly nonlinear with time, and as a consequence, both the length scale and amplitude of the concentration fluctuations grow with time. In the late stage of SD, the amplitude of concentration fluctuations reaches an equilibrium value, but the size of the phase-separated structure keeps growing with time[2].

Scattering theory

Figure 1 shows the experimental setup in this work. The O_z axis is normal to the film surface O_{xy} and parallel to both the axis of the uniaxial compression and the propagation direction of the incident beam. The scattered intensity distribution $I_\perp$ on the detector plane set perpendicular to O_z-axis is circularly symmetric with respect to the incident beam axis,

$$I_\perp(q_x, q_y, t) = I_\perp(q_\perp, t) = K_1\langle\eta^2\rangle q_{m\perp}^{-2}(t) q_{m\parallel}^{-1}(t) S_\perp(q_\perp/q_{m\perp}, t) \quad (2)$$

where $q_k (k = x, y)$ are the components of the scattering vector $\mathbf{q}$ along k-th direction on the detector plane. $q_{m\perp}$ and $q_{m\parallel}$ are the components of the characteristic scattering vector (the scattering vector at the maximum scattered intensity) $\mathbf{q}_m$ perpendicular and parallel to the compression axis, respectively.

$$q_{mz} \equiv q_{m\parallel} \quad (3)$$

$$q_{mx} = q_{my} \equiv q_{m\perp} \quad (4)$$

and

$$q_\perp \equiv (q_x^2 + q_y^2)^{1/2} \quad (5)$$

K_1, $\langle\eta^2\rangle$ and $S_\perp(q_\perp/q_{m\perp}, t)$ are proportionality constant, mean-squared refractive index fluctuations of our systems and scaling function on the detector plane at a given time, respectively. The magnitude of $\mathbf{q}_\perp(q_\perp)$ is defined by

$$q_\perp = (4\pi/\lambda)\sin(\theta/2) \quad (6)$$

with λ and θ being the wavelength of light and scattering angle both in the medium, respectively.

The corresponding integrated intensity at time t, $Q_\perp(t)$, on the detector plane is given by[1]

$$Q_\perp(t) \equiv \int_0^\infty I(q_\perp) q_\perp \mathrm{d}q_\perp = K_2\langle\eta^2\rangle q_{m\parallel}^{-1}(t) \int_0^\infty S_\perp(x, t) x \mathrm{d}x \cong K_3\langle\eta^2\rangle q_{m\parallel}^{-1}(t) \quad (7)$$

with

$$x \equiv q_\perp/q_{m\perp} \quad (8)$$

The scaled structure factor on the detector plane is defined by

$$F_\perp(x, t) \equiv I_\perp(x, t) q_{m\perp}^2(t) = K_4\langle\eta^2\rangle q_{m\parallel}^{-1}(t) S_\perp(x, t) \quad (9)$$

Hereafter we suppress the subscript $\perp$ in $q_\perp$ for the sake of convenience.

Experimental

Samples. PB and SBR were polymerized by living anionic polymerization and had a narrow molecular weight distribution. SBR contains 80 wt% butadiene and has number average molecular weight (M_n) of 1.00×10^5 and $M_w/M_n = 1.18$ (M_w being the weight average molecular weight). PB has $M_n = 1.60 \times 10^5$ and $M_w/M_n = 1.16$. Fractions of *cis*, *trans* and vinyl linkages of the butadiene part as measured by i.r. spectroscopy are 0.16, 0.23 and 0.61 for SBR, and 0.19, 0.35 and 0.46 for PB.

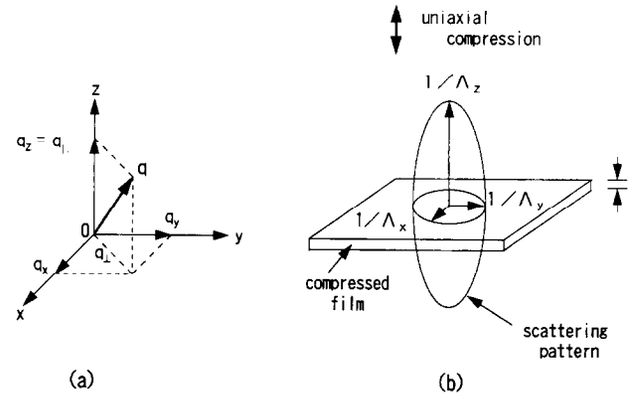

Figure 1 Coordinate system used in this work (a) and the scattering intensity distribution after the compression (b)

Preparation of mixture. Binary mixtures of SBR/PB = 70/30 (v/v) were dissolved into a dilute solution of toluene (7 wt% polymer solution). The 0.15 mm thick film specimens were obtained by evaporating the solvent at natural rate at about 25°C in a petri dish. The film specimen thus obtained was further dried under vacuum for more than one week at room temperature.

The film specimen prepared was homogenized by applying 'Baker's transformation' at room temperature; i.e. by the repeated folding and pressing over many times as reported earlier[4]. The homogenized specimens were quickly sandwiched between two glass plates with a corresponding spacer and were subjected to the light scattering experiments.

Methods of uniaxial compression. The uniaxial compression was performed on the films (designated as *as-prepared film specimens*) which was first subjected to homogenization and then to isothermal demixing for $t_i = 15$–44 min at 60°C, followed by rapid cooling to 25°C. The *as-prepared film* thus obtained was compressed at 25°C after rapidly changing a spacer into a thinner spacer with a half of the original sample thickness by putting a weight of 10 kg on the top of the glass plate. The compression ratio γ_p was fixed to 1/2. We designate the uniaxial compression with $\gamma_p = 1/2$ as '1/2-uniaxial-compression' for the sake of convenience. The weight was then released, the samples were brought back to temperature enclosure controlled at 60°C and immediately subjected to light scattering experiments. The time spent between the end of demixing process at 60°C and the compression process at 25°C and that between the compression process and the onset of the light scattering experiment at 60°C after the compression are negligibly short compared with the time scale of SD process so that they hardly affect the results we discuss here. There was no recovery in the sample dimension

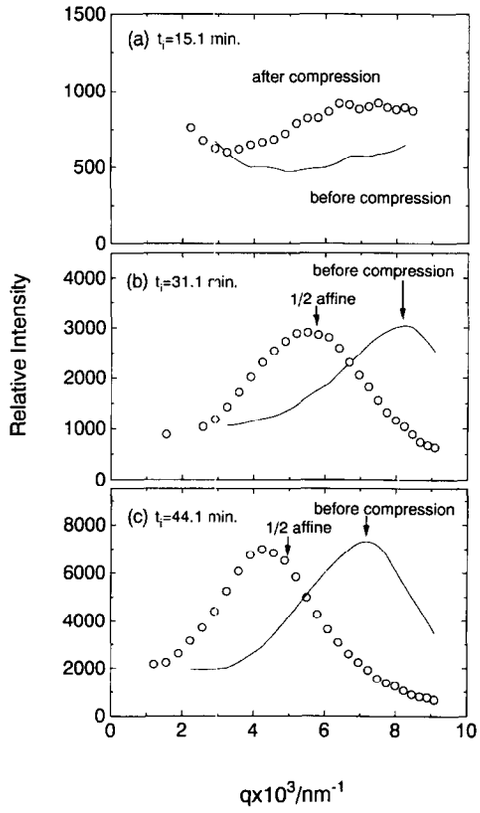

Figure 2 Light scattering profile for a film that was first homogenized and then demixed by annealing at 60°C for t_i = 15.1 (a), 31.1 (b) and 44.1 min (c). The profiles shown by straight lines are obtained immediately before the compression ($\gamma_p = 1$) and those shown by circles immediately after the 1/2-uniaxial-compression at 25°C. The arrows marked with '1/2 affine' indicate the peak position expected for isochoric affine deformation with $\gamma_p = 1/2$

after the removal of the weight and the stress relaxed completely before applying the new folding–pressing in the Baker's transformation process and before applying the light scattering experiment after the compression.

Methods of observation. The isothermal demixing process was investigated by means of the time-resolved light scattering technique. A He–Ne laser of 15 mW power was used as an incident beam source. The compressed film was set into a metal block, with two windows for the incident and scattered beam sides, preheated at a demixing temperature at 60°C. The scattering profiles were observed in one direction on the detector plane set perpendicular to the uniaxial compression axis.

Experimental results

Effects of uniaxial compression on phase-separated domains. Figure 2 shows the light scattering profile from the *as-prepared film* which were first homogenized and demixed at 60°C for t_i = 15.1 (a), 31.1 (b) and 44.1 min (c) (straight line) together with those from the *as-prepared films* subsequently subjected to the 1/2-uniaxial-compression at 60°C (circles). The scattering maximum arising from a periodic concentration fluctuation, which was developed in the homogenized films via SD, shifts toward a smaller q with the compression, indicating that the phase-separated domains expanded to the direction perpendicular to the uniaxial compression axis, as clearly seen in parts (b) and (c). The arrows marked

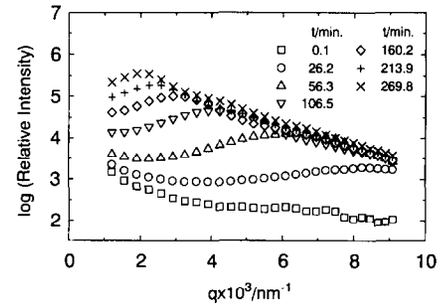

Figure 3 Time evolution of the scattering profiles, on a semi-logarithmic scale, during the isothermal demixing at 60°C for the homogenized film. The time $t = 0$ was taken immediately after the homogenization process and onset of phase separation

with 'before compression' and '1/2 affine' designate, respectively, the peak position observed for the sample before the compression and that expected for the case in which the compression induces isochoric affine deformation. The shift seems to be approximately described by the affine deformation[1]. For a short phase-separation time (t_i = 15.1 min; corresponds to the early stage SD as will be clarified later), the scattering profile immediately before the uniaxial compression could not be observed because the value $q_{m\perp}$ before the compression exists at a high q value outside our experimental window. However, after the compression, $q_{m\perp}$ came inside the window of our observation. The compression was imposed on the film for a few minutes. This time is much shorter than that of the structural evolution driven by the thermodynamic driving force, but is longer than that for stress relaxation and for the relaxation of molecular orientation.

Time evolution of scattering profile after uniaxial compression. Figure 3 shows the time evolution of light scattering profiles at 60°C, on a semi-logarithmic scale, from the film after the homogenization but with no compression ($t_i = 0$ and $\gamma_p = 1$). As time elapses, a scattering maximum appears and the maximum intensity increases and the scattering vector $q_{m\perp}$ at the maximum intensity shifts toward small q. The phenomenon which reflects the coarsening of phase-separated domains was described well previously[5–7].

Figure 4 shows the time evolution of light scattering profiles after the compression ($\gamma_p = 1/2$) at $t = t_i$ = 15.1 (a), 31.1 (b), and 44.1 min (c). Here the time t was set equal to zero immediately after the homogenization and onset of the phase separation at 60°C. Let us briefly summarize here once again our experimental procedure to avoid confusion. The films were first homogenized and then subjected to the isothermal demixing at 60°C for a time period t_i equal to 15.1–44.1 min, then they were quenched to 25°C and subjected to the 1/2-uniaxial-compression at 25°C; they were finally quickly transferred back to the heater block precontrolled at 60°C for further phase separation. In these figures, straight lines correspond to the scattering profiles at $t = t_i$ immediately before the uniaxial compression, and the profiles shown by squares are those immediately after the compression. After imposing the uniaxial compression, the following changes in the scattering profile was observed: (i) at a short annealing time (t_i = 15.1 min; corresponds to the early stage of SD), the scattering intensity immediately after the uniaxial compression seems to be slightly larger

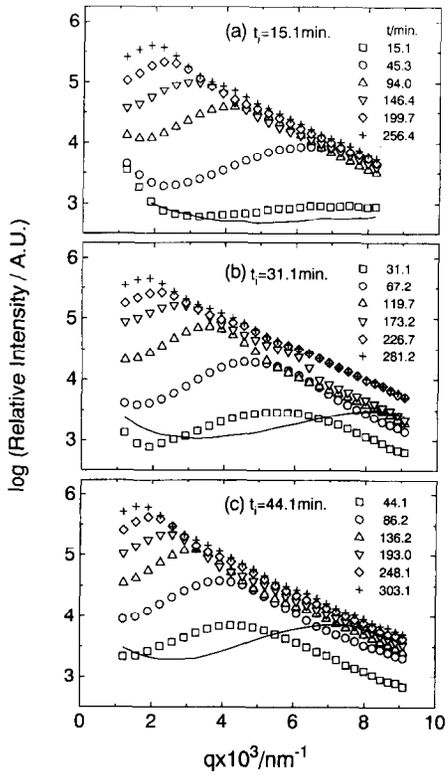

Figure 4 Time evolution of the scattering profiles for the compressed films ($\gamma_p = 1/2$) at $t_i = 15.1$ (a), 31.1 (b), and 44.1 min (c) at 60°C. The films which were first homogenized and then subjected to the time-resolved LS experiment at 60°C (time zero is set right after the homogenization, i.e. the onset of SD at 60°C), followed by quenching to 25°C where the uniaxial compression was imposed on the film, and finally quickly transferred to the heater block preheated at 60°C for further phase separation. The scattering profiles shown by squares are immediately after the uniaxial compression, while those shown by straight lines are immediately before the compression

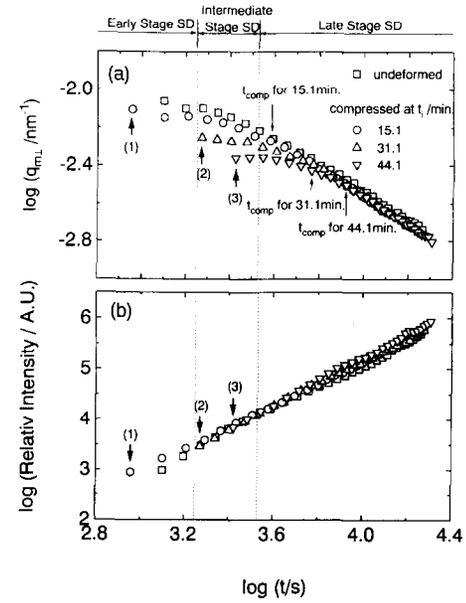

Figure 5 Time changes in the scattering vector at the maximum intensity $q_{m\perp}(t; t_i, \gamma_p)$ (a) and the maximum scattered intensity $I_{m\perp}(t; t_i, \gamma_p)$ (b), on a double logarithmic scale, from films subjected to the 1/2-uniaxial-compression at various t_i's at 60°C

compared with that immediately before the compression (*Figure 4a*). (ii) at the intermediate stage of SD ($t_i = 31.1$ and 44.1 min), the scattering maximum shifts toward a smaller q value without a significant change in the maximum intensity, (iii) in the earlier time of the phase separation process after the compression, the scattering intensity increases with time without a significant change in the value $q_{m\perp}$.

Analysis and discussion

Phase separation after uniaxial compression: time evolution of characteristic wave number $q_{m\perp}$. *Figure 5a* shows the time changes in the scattering vector $q_{m\perp}(t; t_i, \gamma_p)$ on the detector plane for undeformed case (squares) ($t_i = 0, \gamma_p = 1$), for deformed films ($\gamma_p = 1/2$) with $t_i = 15.1$ (circles), 31.1 (triangles) and 44.1 min (inverted triangles) on a double logarithmic scale, all at 60°C. Time evolution of the $q_{m\perp}$ for undeformed case was described in our earlier study and will be briefly summarized in the next section[6]. The values $q_{m\perp}(t; t_i, \gamma_p)$ for the compressed films suddenly decrease toward smaller values with imposing uniaxial compression at time t_i as indicated by the arrows marked by (1)–(3), and stays essentially constant for a time. Then they slowly decrease until a certain time t_{comp}, beyond which the values $q_{m\perp}$ for the samples with and without the compression deformation become identical and decrease with t at the same rate. The time t_{comp} appears to depend on t_i; the longer the phase separation time, the longer the time t_{comp}. Thus the memory effect of the uniaxial compression decays during the ordering process after the compression at the level of $q_{m\perp}(t = t_{comp}; t_i = 0, \gamma_p = 1) \cong q_{m\perp}(t = t_{comp}; t_i > 0, \gamma_p = 1/2)$ and thereafter the coarsening depends purely on temperature.

Figure 5b shows the time changes in the maximum scattered intensity $I_{m\perp}(t; t_i, \gamma_p)$ on the detector plane for the undeformed film (squares) ($t_i = 0$ and $\gamma_p = 1$), that for deformed films ($\gamma_p = 1/2$) with $t_i = 15.1$ (circles), 31.1 (triangles) and 44.1 min (inverted triangles) on a double logarithmic scale, all at 60°C. The results indicate that the maximum scattering intensity $I_{m\perp}$ was not affected by the uniaxial compression. The reason was described in the previous paper[1].

Phase separation after uniaxial compression: linear analysis. At an earlier time after the uniaxial compression $q_{m\perp}(t; t_i, \gamma_p)$ appears to be constant, almost independent of time. Thus we tried to apply the linear analysis of SD to the time evolution of $I_\perp(q, t_a)$ in this time domain where t_a is defined as the time spent after the compression ($0 \leqslant t_a < t_{comp}$). Hereafter, we suppress the subscript $\perp$ in $I_\perp$ for simplicity. The linearized theory gives

$$I_\perp(q_\perp, t_a) \equiv I(q, t_a) = I(q, t_a = 0) \exp[2R(q)t_a] \quad (10)$$

where $R(q)$ is a growth rate of the Fourier mode of the concentration fluctuations with wave number q after the uniaxial compression. $R(q)$ is determined from the slope of ln $I(q, t_a)$ vs t_a. It should be noted that $I(q, t_a)$, $I(q, t_a = 0)$ and $R(q)$ generally depend on t_i and γ_p. In a small q regime where $qR_0 \ll 1$ (R_0 being the unperturbed end-to-end distance of polymers) it can be shown that the $R(q)$ is given by

$$R(q) = q^2 D_{app}[1 - q^2/2q_m^2(0)] \quad (11)$$

where D_{app} is the mutual diffusivity of polymer mixtures and $q_m(0)$ is the characteristic wave number in the early stage SD. The characteristic parameters $q_m(0)$ and D_{app} for the mixture without deformation were

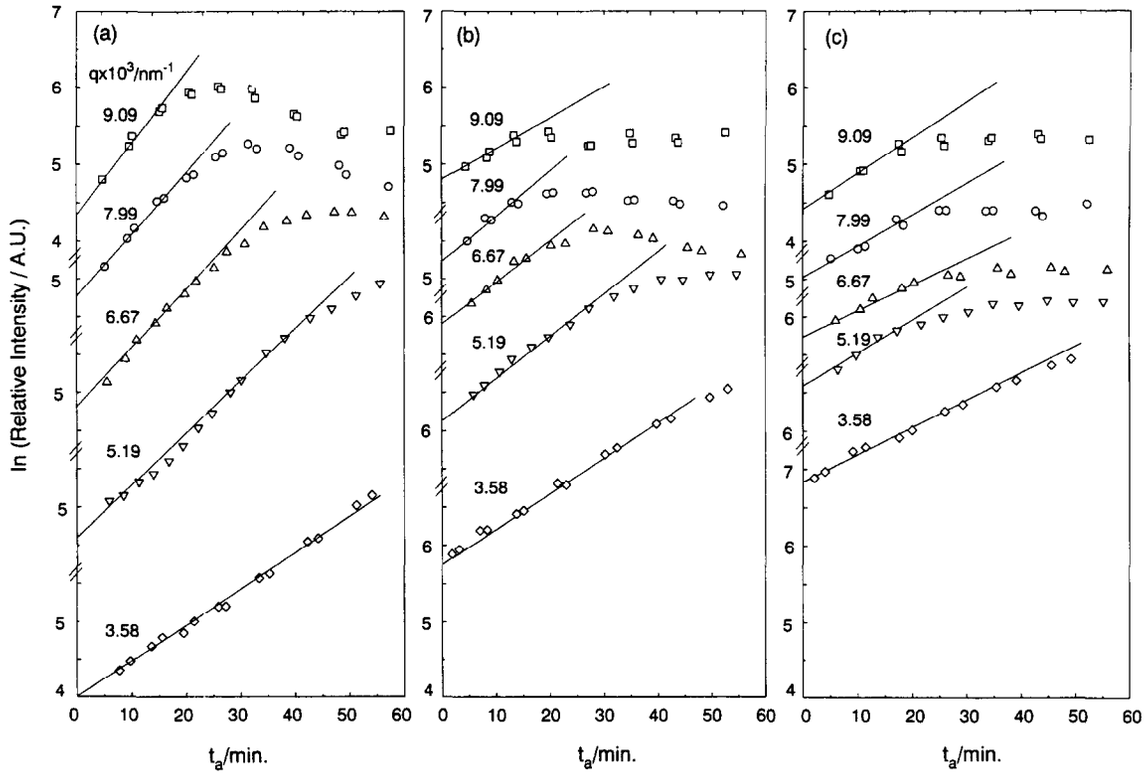

Figure 6 Ln $I_{\perp}(q, t; t_i, \gamma_p)$ vs t_a (t_a; time after the uniaxial compression) for films subjected to the 1/2-uniaxial-compression at 60°C with t_i = 15.1 (a), 31.1 (b) and 44.1 min (c)

obtained in our earlier study[5]: $D_{app} = 27\,nm^2\,s^{-1}$ and $q_m(0) = 9.3 \times 10^{-3}\,nm^{-1}$ at 60°C; the characteristic time $t_c = 430\,s$ where t_c is defined by $t_c \equiv (q_m^2(0)D_{app})^{-1}$ at 60°C.

The time t_i (15.1, 31.1 and 44.1 min) spent for the phase separation before the uniaxial compression, corresponds to the reduced time $\tau = 2.1$, 4.3 and 6.2, where τ is defined as $\tau \equiv t/t_c$. For the polymer mixture studied here, the linear region can be found from 0.1 to 30 min ($\tau \sim 2$: region of the early stage SD) and the crossover time t_{cr} from the intermediate stage SD to the late stage SD is $t_{cr} = 72$ min ($\tau_{cr} = 10.0$)[6]. Therefore, the uniaxial compression was imposed at an early-to-intermediate stage.

Figure 6 shows the variations of logarithmic scattered intensity ln $I(q, t; t_a, \gamma_p)$ with t_a at a various scattering vector q during the demixing at 60°C after the 1/2-uniaxial-compression at t_i = 15.1 (a), 31.1 (b) and 44.1 min (c). As shown in the figure, the scattered intensity increases exponentially with time in the early stage of the ordering process after the compression in the q-range covered in this experiment. The deviation of the intensity increase from the exponential behaviour is seen in the later time, reflecting the shift of the scattering maximum toward smaller q. One can find that the time region where the linearized theory of equation (10) is applicable decreases with an increase of t_i. The q-dependence of the growth rate $R(q)$ in the early time after the compression was estimated on the basis of equation (10). The results obtained are plotted in *Figure 7*.

In the case in which the compression was imposed after a short annealing time (t_i = 15.1 min), the maximum growth rate is found at $q = q_m \cong 7 \times 10^{-3}\,nm^{-1}$ [the arrow marked (a)]. This maximum shifts toward smaller q with increasing the annealing time before the compression as shown by the arrows (a)–(c), and the

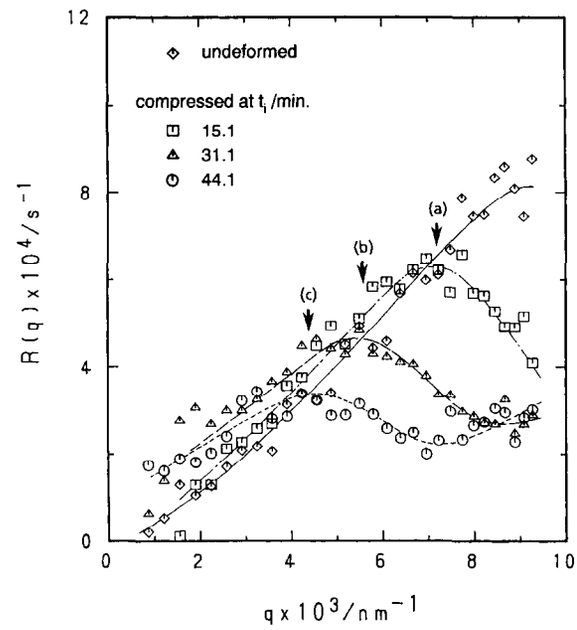

Figure 7 Growth rates of the concentration fluctuations with wave number q $R(q; t_i, \gamma_p)$ for the films subjected to the 1/2-uniaxial-compression at 60°C at t_i = 15.1 (a), 31.1 (b) and 44.1 min (c). Straight line corresponds to undeformed case. The various lines through the data points are for visual guides. The arrows indicate the scattering vectors $q_{m\perp}(t_i, \gamma_p)$ at the maximum scattered intensity immediately after the uniaxial compression

maximum growth rate decreases with increasing the annealing time before the compression. The values q_m shown by the arrows (a)–(c) coincide with those observed in the scattering profiles immediately after the compression and hence reflect the growth behaviour of the dominant mode of the concentration fluctuations after the deformation (see *Figure 4*).

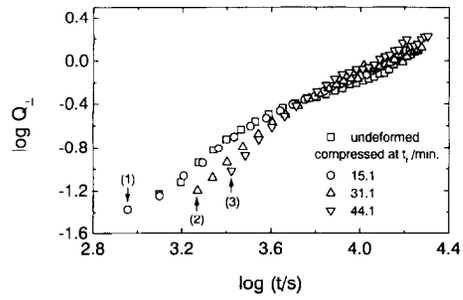

Figure 8 Time changes in the integrated scattering intensity $Q_\perp(t; t_i, \gamma_p)$ on detector plane on a double logarithmic scale, for the films subjected to the uniaxial compression at 60°C after the phase separation for various t_i

$R(q)$ turns out to depend strongly on the initial condition, and this clearly reveals that the ordering process after the compression is a nonlinear process, even though it appears to be superficially linear from view points of the constant $q_{m\perp}$ with time t_a and the exponential growth of $I(q, t_a)$ with t_a. When we compare $R(q)$ for the system subjected to the compression at $t = t_i$ with that for the undeformed system, we note the following points: (i) the shorter the time t_i, the smaller the initial concentration fluctuations that existed for the ordering process after the compression, and hence the smaller the effect of initial fluctuations on $R(q)$, so that the values $R(q)$ at given q's deviate less from those for the undeformed case; (ii) the compression at a given t_i tends to increase slightly $R(q)$ at small q's but decrease strongly at large q's; (iii) $R(q)$ obtained after the compression at $t_i = 44.1$ min tends to show double maxima, one at $q \cong 4.2 \times 10^3\,\mathrm{nm}^{-1}$ and the other at q higher than $10^{-2}\,\mathrm{nm}^{-1}$. The larger q modes are new modes developed after the compression within the pre-existing domains. A similar trend is observed for $R(q)$ obtained after the compression at the shorter t_i's but the new modes developed are expected to be seen at higher q's. This results also suggest that one must be extremely careful about any sorts of initial concentration fluctuations which might exist in specimens when $R(q)$ is analysed in the early stage SD.

Let us next consider how the integrated intensity on the detector plane $Q_\perp(t; t_i, \gamma_p)$ changes with time during the ordering process after the compression. The value $Q_\perp$ is defined in equation (7) but it is actually integrated over $q_\perp$ from $q_{\perp,\min}$ and $q_{\perp,\max}$ which are, respectively, the q values below and above which the integrand goes effectively to zero. $q_{\perp,\min}$ and $q_{\perp,\max}$ taken are $0.5q_{m\perp}$ and $1.5q_{m\perp}$, respectively, where $q_{m\perp}$ depends on t_i and t_a.

Figure 8 shows, on a double logarithmic scale, the integrated intensity $Q_\perp(t; t_i, \gamma_p)$ as a function of time for the films annealed for various periods of time t_i before compression. The results indicate that, at an earlier time after the uniaxial compression, the level of the $Q_\perp(t; t_i, \gamma_p)$ was affected by t_i. The compression after a short annealing time (at $t = t_i = 15.1$ min; corresponding to the early stage SD) hardly affects $Q_\perp(t; t_i, \gamma_p)$ so that its time evolution is nearly identical to $Q_\perp$ for the undeformed specimen. This is intuitively understood as a consequence of a small memory effect. On the other hand, the compression at $t_i \geq 31.1$ min (corresponding to the intermediate stage SD) lowers the level of the $Q_\perp(t; t_i, \gamma_p)$ relative to the undeformed case as shown by the arrows marked (2) and (3). In order to interpret this result, we should note the following two pieces of evidence: (i) as clarified in our previous experimental analysis[1], the uniaxial compression does not essentially change $\langle \eta^2 \rangle$ and $S_\perp(x)$ but (ii) decreases $q_{m\parallel}^{-1}$ or increases $q_{m\parallel}$. This evidence and equation (7) clarifies the observed result. The increase of $Q_\perp$ with time after the compression is due to a further increase of both $\langle \eta^2 \rangle$ and $q_{m\parallel}^{-1}$ with t in the ordering process after the compression. Note that $q_{m\parallel}$ increases upon imposing compression but decreases with time after the compression in the ordering process[1]. Hence $q_{m\parallel}^{-1}$ increases with time after the compression. However, in the late stage the increase is only due to the increase of $q_{m\parallel}^{-1}$. Again the memory effect of the uniaxial compression decays at a long enough time after the uniaxial compression. As a result the coarsening process depends only on the phase-separation temperature.

Phase separation after uniaxial compression: scaled structure factor. Here we analysed the scaled structure factor. If the time evolution of the scattering pattern obeys the dynamical scaling law, then the time evolution of the scattering function $I(q, t; t_i, \gamma_p)$ after the compression is given in terms of the universal scaling function S. From equations (7) and (9), the reduced scaled structure factors $\bar{F}(x)$ is defined by

$$\bar{F}(x, t) \equiv F_\perp(x, t)/Q_\perp(t) = K_5 S_\perp(x, t) \qquad (12)$$

where we suppressed $\perp$ in $\bar{F}_\perp(x)$ for the sake of simplicity.

Figures 9a–c show the reduced scaled structure factor

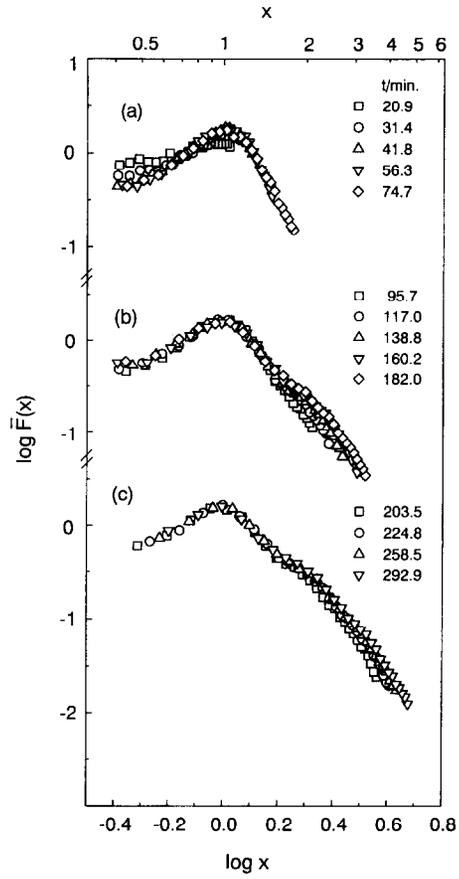

Figure 9 Reduced scaled structure factor $\bar{F}(x)$ on a double logarithmic scale at 60°C with $x \equiv q/q_{m0}$ for the undeformed film ($t_i = 0$ and $\gamma_p = 1$)

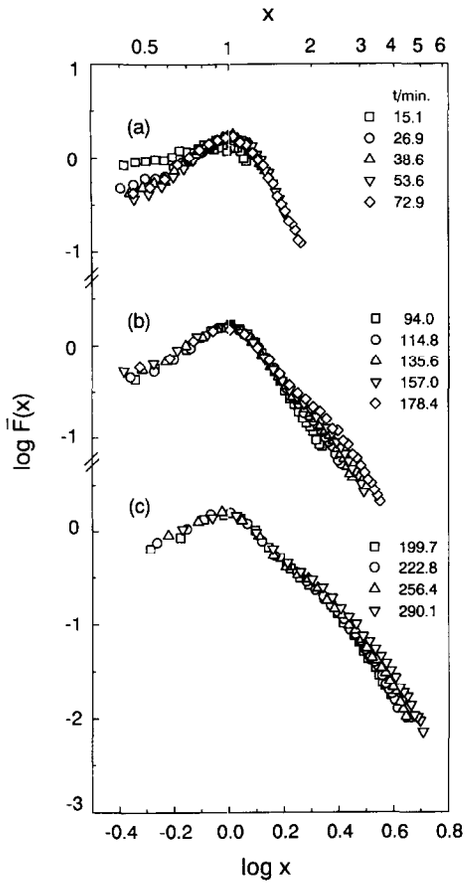

Figure 10 Reduced scaled structure factor $\bar{F}(x)$ after the 1/2-uniaxial-compression, on a double logarithmic scale, at 60°C with $x \equiv q/q_{m\perp}$ for the film compressed at $t_i = 15.1$ min

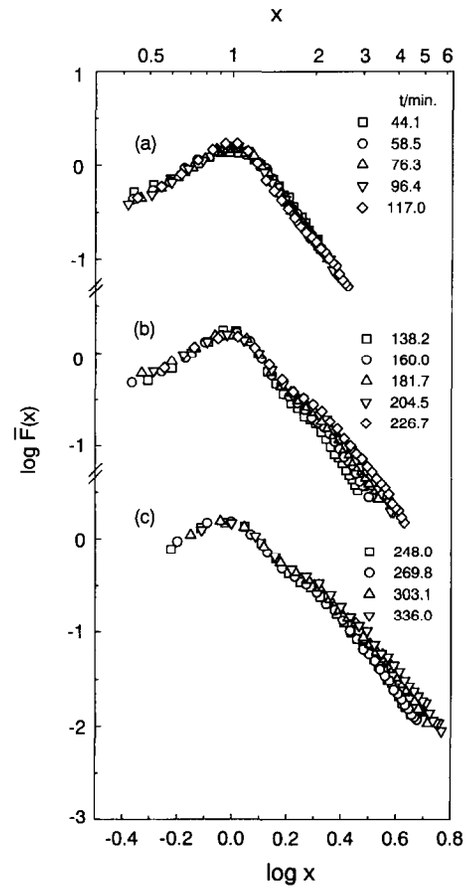

Figure 11 Reduced scaled structure factor $\bar{F}_\perp(x)$ after the 1/2-uniaxial-compression, on a double logarithmic scale, at 60°C with $x \equiv q/q_{m\perp}$ for the film compressed at $t_i = 44.1$ min

$\bar{F}$ for the undeformed films (with $t_i = 0$ and $\gamma_p = 1$). Note that the crossover time t_{cr} between the intermediate stage and the late stage was 72 min, so that part a corresponds to the structure factors in the intermediate stage and parts b and c to those in the late stage. Note that even in the intermediate stage the scaled structure factor $\bar{F}$ normalized with $Q_\perp \sim \langle\eta^2\rangle$ is nearly universal with t except for those at 20.9 and 31.4 min, indicating that the global structure manifested by $\bar{F}$ is nearly dynamically self-similar: only $\langle\eta^2\rangle$ and the length parameter $q_{m\perp}^{-1}$ increase with time. The structure factor significantly becomes sharp at the earlier phase. A high order maximum was observed at $x \cong 2$ in parts b and c. $\bar{F}(x)$ have the asymptotic behavior x^n with $n \cong -6$ in the range of $1 < x < 2$ and -4 in the range of $x > 2$ as described earlier[7]. The domains with a sufficiently uniform spatial periodicity are essential to the high order peak in $\bar{F}(x)$. The increase of $\bar{F}(x)$ at $x > 2$ in part b is due to a narrowing of the interface thickness t_I (late stage I)[8].

Figures 10a–c show the reduced scaled structure factor $\bar{F}(x)$ after the 1/2-uniaxial-compression at $t = t_i = 15.1$ min at 60°C. The time change in the scale structure factors (curves b and c) after the compression is essentially identical to that of the undeformed case (parts b and c in *Figure 9*). Thus in the time domain covered by parts b and c the uniaxial compression appears to change primarily the characteristic wave numbers $q_{m\perp}(t)$ and $q_{m\parallel}(t)$. Note that the time t_{comp} beyond which the evolution of $q_{m\perp}(t; t_i > 0, \gamma_p = 1/2)$ is equal to that of $q_{m\perp}(t; t_i = 0, \gamma_p = 1)$ is 73 min. This was judged only from the global parameter $q_{m\perp}(t; \gamma_p)$ (*Figure 5*), i.e. from a particular length scale of $q_{m\perp}^{-1}$. The structure factors shown in *Figures 9* and *10* illuminate a more complete picture: they reveal that the structures obtained with and without the uniaxial compression become identical at all length scales after $t \geq t_{comp}$.

Figures 11a–c show the reduced scaled structure factor $\bar{F}(x)$ after the 1/2-uniaxial-compression at $t = t_i = 44.1$ min at 60°C. The time t_{comp} judged from *Figure 5* was 117 min. The time change in the scaled structure factor after the compression (curves b and c) is also essentially identical to that of the undeformed case (*Figure 9*). In the time domain covered in part c the memory effect of the uniaxial compression has essentially decayed at all length scales.

Conclusions

Light scattering experiments have been performed on the phase separation process of the binary mixture of SBR and PB with a near-critical composition subjected to the 1/2-uniaxial-compression at various times t_i after the onset of phase separation. The scattering profiles perpendicular to the compression axis were observed and analysed. Immediately after the uniaxial compression on the film which was first homogenized and then demixed at 60°C for 15–44 min, the scattering vector at the maximum intensity $q_{m\perp}(t_i, \gamma_p = 1/2)$ shifted toward smaller q, essentially according to isochoric affine deformation. After the uniaxial compression, the time change in the scattering vector $q_{m\perp}(t; t_i, \gamma_p = 1/2)$ was considerably slowed down, and essentially remains

constant with time. As time elapses $q_{m\perp}(t; t_i, \gamma_p = 1/2)$ approaches the value $q_{m\perp}(t; t_i = 0, \gamma_p = 1)$, the time change in the characteristic wave number in the absence of the compression, indicating the memory effect of the uniaxial compression on $q_{m\perp}(t; t_i, \gamma_p = 1/2)$ decays with time. On the other hand, the time evolution of the maximum scattering intensity $I_{m\perp}(t; t_i, \gamma_p)$ was not affected by the uniaxial compression. This is because the changes in $\langle \eta^2 \rangle$, $q_{m\perp}^{-2} q_{m\parallel}^{-1}$ and $S_\perp(x)$ with time are hardly affected by the compression. In an earlier time after the uniaxial compression, $I_\perp(q; t; t_i, \gamma_p)$ was observed to increase exponentially with time spent after the uniaxial compression t_a. The maximum growth rate of the concentration fluctuation $R_m(t_i, \gamma_p)$, which was characterized from a slope of the ln $I_\perp(q, t; t_i, \gamma_p)$ vs t plots, decreases with increase of the phase separation time t_i before 1/2 compression. The increase of t_i implies the formation of bigger concentration fluctuations in both amplitude and spatial extension after the compression, as initial conditions for phase separation after the compression. The results clearly revealed that the ordering process is intrinsically nonlinear and that the growth rates of the new modes of the concentration fluctuations which developed after the compression strongly couple with the pre-existing modes. These intriguing features are consistent with our earlier experiments with a fixed t_i but varying γ_p. Time change in the scaled structure factor was determined as a function of t_i. The change for the compressed film is essentiallly identical to that of the undeformed case, indicating that the compression changes only the characteristic length scales $q_{m\parallel}^{-1}$ and $q_{m\perp}^{-1}$ but not the shape of the phase separating structure itself. It was also illuminated that sometime after the compression (at $t > t_{comp}$) the effects of the compression on the phase-separating domain structures completely disappear: the time change in the domain structures depends only on temperature; the structures developed with or without the compression become identical at all length scales. This also highlights a consequence of the nonlinear dynamics.

Acknowledgements

The authors express their thanks to Japan Synthetic Rubber Co. Ltd for providing the samples. This work was partially supported by a scientific grants from Japan Synthetic Rubber Co. Ltd and Yokohama Rubber Co. Ltd Japan.

References

1. Hashimoto, T. and Izumitani, T., *Macromolecules*, 1996, **29**, 8117.
2. Hashimoto, T., Itakura, M. and Hasegawa, H., *J. Chem. Phys.*, 1986, **85**, 6118; Hashimoto, T., Itakura, M. and Shimidzu, N., *J. Chem. Phys.*, 1986, **85**, 6773.
3. Cahn, J. W. and Hilliad, J. E., *J. Chem. Phys.*, 1958, **28**, 258; Cahn, J W., *J. Chem. Phys.*, 1965, **42**, 93; de Gennes, P. G., *J. Chem. Phys.*, 1980, **72**, 4756.
4. Hashimoto, T., Izumitani, T. and Takenaka, M., *Macromolecules*, 1989, **22**, 2293.
5. Izumitani, T. and Hashimoto, T., *J. Chem. Phys.*, 1985, **83**, 3694.
6. Izumitani, T., Takenaka, M. and Hashimoto, T., *J. Chem. Phys.*, 1990, **92**, 3213.
7. Takenaka, M., Izumitani, T. and Hashimoto, T., *J. Chem. Phys.*, 1990, **92**, 4566.
8. Hashimoto, T., Takenaka, M. and Jinnai, H., *J. Appl. Cryst.*, 1991, **24**, 457; Takenaka, M. and Hashimoto, T., *J. Chem. Phys.*, 1992, **96**, 6177.